
ProteinN: Intrinsic-Extrinsic Convolution and Pooling for Scalable Deep Protein Analysis

Pedro Hermosilla
Ulm University

Marco Schäfer
Tübingen University

Matěj Lang
Masaryk University

Gloria Fackelmann
Ulm University

Pere Pau Vázquez
Polytechnic University of Catalonia

Barbora Kozlíková
Masaryk University

Michael Krone
Tübingen University

Tobias Ritschel
University College London

Timo Ropinski
Ulm University

Abstract

Proteins perform a large variety of functions in living organisms, thus playing a key role in biology. As of now, available learning algorithms to process protein data do not consider several particularities of such data and/or do not scale well for large protein conformations. To fill this gap, we propose two new learning operations enabling deep 3D analysis of large-scale protein data. First, we introduce a novel convolution operator which considers both, the intrinsic (invariant under protein folding) as well as extrinsic (invariant under bonding) structure, by using n -D convolutions defined on both the Euclidean distance, as well as multiple geodesic distances between atoms in a multi-graph. Second, we enable a multi-scale protein analysis by introducing hierarchical pooling operators, exploiting the fact that proteins are a recombination of a finite set of amino acids, which can be pooled using shared pooling matrices. Lastly, we evaluate the accuracy of our algorithms on several large-scale data sets for common protein analysis tasks, where we outperform state-of-the-art methods.

1 Introduction

Proteins enable specific biological functions essential for all living organisms and hence play a key role when investigating the most fundamental questions in the life sciences. Consequently, it is of high importance to enable end-to-end learning on proteins, such that this domain can benefit from modern learning technologies to the same degree as other disciplines did in the last years.

Proteins are composed of amino acid chains, which result in a multi level structure. The *primary* structure is given by the sequence of amino acids, which are connected through covalent bonds and define a protein's backbone. Hydrogen bonds between residues form the *secondary* structure, which forms substructures such as α -helices and β -sheets. The *tertiary* structure, resulting from protein folding, expresses the 3D spatial arrangement. Lastly, the *quarternary* structure is given by the interaction of multiple amino acid chains.

We propose a novel end-to-end protein learning methodology to explicitly incorporate this multi-level structure. Primary, secondary, and tertiary structures are directly captured by protein structure data. We show how a multi-graph data structure can capture the primary and secondary structures effectively (Sec. 3), by considering covalent and hydrogen bonds, while the tertiary structure can be represented by a spatial data structure. As chain bindings affect the tertiary positions, the quaternary structure is captured implicitly. Therefore, it does not have to be considered explicitly during learning. Next,

we propose convolutions to use both intrinsic (bonds) and extrinsic (spatial arrangement) distances (Sec. 4). Protein sizes range from less than one hundred to tens of thousands of amino acids [6]. We propose a protein-specific pooling operation that enables hierarchical grouping on such sizes (Sec. 5.2). The proposed operations are differentiable, conceptually simple, and allow for an efficient GPU implementation. We will evaluate the performance of our contributions in a deep architecture and show that we outperform the state-of-the-art often by a large margin (Sec. 6).

2 Related Work

Molecule learning. The seminal works by Duvenaud et al. [11] and later by Kearnes et al. [26], Gilmer et al. [15], as well as Klicpera et al. [28], applied different learned operations to molecular analysis for quantum chemistry. In particular, the approach of Duvenaud et al. [11] was already convolutional, but only in the sense that the same fingerprint is applied in multiple places. Regrettably, these ideas do not scale to the demands of proteins which are two orders of magnitude larger than what they can cope with. Without pooling, information from one end of a long protein chain will “travel” too slowly in common message passing to be useful. For a survey on general molecular learning, a reader may wish to consult Elton et al. [12], while in the following, we will focus only on protein-specific solutions.

Protein learning. For learning on proteins, many early attempts have focused on the primary structure only, effectively reducing the complex spatial and topological structure to a sequence of amino acids [32]. Hence, the problem becomes a simple 1D convolution. While this is a well-motivated protein-specific view on the problem, as sometimes only sequence data is available, it does not consider the other levels of structure, which directly influence protein functions. Borgwardt et al. [5] stressed that a protein has different types of bonds and, in a non-learned architecture, supported both. We enable this using tunable operations. A range of methods [2, 43, 47, 31, 8, 46, 25] have sampled proteins to regular volumetric 3D representations to facilitate classification. This is attractive, as such a 3D grid allows for the application of all operations developed for 2D images, such as pooling and multi-resolution techniques. Unfortunately, grids do not scale well to fine structures or many atoms. As our approach works end-to-end on the topology and geometry of the full protein at comparable speed, our results show substantial improvements. Gligorijevic et al. [16] use graph neural networks (GNNs) to analyze proteins. They show that avoiding discretization can be beneficial and still scale to relevant proteins. We show how multi-graphs, convolutions that respect these, and pooling, all specific to proteins, improve the published results. Another view is taken by Ingraham et al. [24], which suggests addressing proteins from a generative modelling perspective. No applications to more mundane tasks, such as classification, are demonstrated.

Convolutions. Many attempts to generalize convolutions from regular domains to less structured ones exist [20, 38, 27, 18, 28, 13, 52, 34], as reviewed by Wu et al. [50]. To our knowledge, no such convolution has considered using multiple distances in order to combine multiple intrinsic distances with one extrinsic distance. Other approaches used high-order neighborhoods [36] based on shortest-path [21] or Quantum Walks [54]. Our method differs from those since we define our neighborhood based on the Euclidean distance and compute the geodesic distances on a multi-graph as additional dimensions to our kernel. Knyazev et al. [29] use different graph edge types, but learn those edges, while for us they are part of our input data.

Pooling. While pooling is easy in images, it is much harder to do in graphs. Ying et al. [51] suggested the intriguing idea to learn the pooling operation itself. Regrettably, this approach represents and operates on connectivity matrices, requiring quadratic storage, which defies its application to large proteins. Gao and Ji [14] proposed a way to implement U-Net [44] on graphs. They suggested a learning-based method to remove nodes of the graph, which would result in a set of disconnected sub-graphs in the context of proteins. They report results on “protein interaction graphs”, which are smaller and not to be mistaken with proteins. Another inspiring suggestion by Lee et al. [33] is to use attention to select which information should be pooled. Unfortunately, as with the previous method, this would also lead to disconnected sub-graphs. Similar approaches based on the Fourier Transform (FT) [35] do not scale to relevant atom numbers. The edge contraction pooling suggested by Diehl [9] is another creative and simple-to-implement idea, inspired by edge collapsing as done in computer graphics [23] and hence potentially scalable. We avoid the sequential pooling by performing the same pooling on every repeating amino acid.

Scalable unstructured learning. In computer vision and computer graphics, scalability is a pressing issue when dealing with millions of 2D pixels or 3D points. Hence, specific methods [41, 42, 17, 3, 22, 45] have been proposed that can accommodate large inputs by using efficient data structures. Our approach extends these ideas to support protein-specific requirements, while at the same time retaining their efficiency.

3 Multi-Graph Protein Representation

To take into account the protein primary and secondary structure during learning, we propose to represent proteins as a multi-graph $\mathcal{G} = (\mathcal{N}, \mathcal{E}_1, \dots, \mathcal{E}_{n_b})$, where atoms are represented by nodes \mathcal{N} and bonds are represented by sets of edges $\mathcal{E}_1, \dots, \mathcal{E}_{n_b}$, whereby n_b is the number of edge types to consider. Every node $N = (\mathbf{x}, \mathbf{f})$ stores a position $\mathbf{x} \in \mathbb{R}^3$, representing the protein’s extrinsic geometry as well as features $\mathbf{f} \in \mathbb{R}^n$. The particular choice of features in our experiments is detailed in Sec. 6.1.

While this multi-graph representation can be used in various ways for proteins or other molecules, we use it to capture two kinds of bonds: covalent bonds to capture a protein’s primary structure and hydrogen bonds to capture the secondary structure. \mathcal{E}_1 uses the covalent bonds \mathcal{E}_c . Hydrogen bonds \mathcal{E}_h form a sparse set of additional connections. For meaningful distances along the graph, we hence use $\mathcal{E}_2 = \mathcal{E}_c \cup \mathcal{E}_h$.

4 Intrinsic-Extrinsic Protein Convolution

Our intrinsic-extrinsic protein convolution maps a multi-graph of fixed structure with an input feature size per node to another multi-graph with the same structure, but, in general, different feature dimensions. The key idea is to enable convolutions to pick up multiple invariances. Fig. 1 shows how similar geometry but different topology (bonding) can indicate a change in functionality, while the same topology, but different geometry (folding) can also change the meaning. Hence, we use both intrinsics and extrinsics.

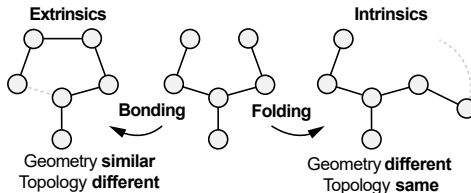


Figure 1: Intrinsic and extrinsic invariance resulting from bonding and folding on a hypothetical protein structure.

To this end, we provide to the convolution kernel $\kappa(\tau_e, \tau_{i,1}, \tau_{i,2}, \dots, \tau_{i,n_b}) \in \mathbb{R}^{1+n_b} \rightarrow \mathbb{R}^{n_f}$ both the extrinsic distance τ_e in the 3D Euclidean space, as well as multiple intrinsic distances $\tau_{i,1}, \tau_{i,2}, \dots$, one for each of the n_b types of edges. The convolution, performed independently for every node, is illustrated on a hypothetical protein in Fig. 2, where two edge types, blue and green, are shown.

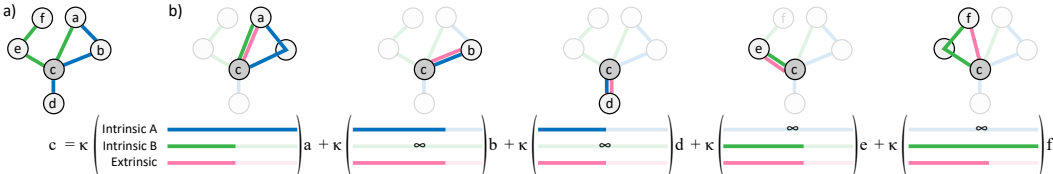


Figure 2: Intrinsic-extrinsic convolution on a multi-graph with a blue and a green bond (a). This convolution has five summands (b). For each summand, the extrinsic (pink) and two intrinsic (blue and green) distances are input into the kernel and shown below.

In practice, the summation is restricted to a receptive field for both computations, of intrinsic and extrinsic distances, whereby we assume a fixed extrinsic radius and a fixed number of hops for intrinsics. We use shortest-path distances. Also, several different options exist to represent the kernel function, ranging from linear functions [17] to RBFs [3] and MLPs [22]. While later we will propose a neighborhood and kernel representation, our idea is independent of that choice.

5 Hierarchical Protein Pooling

Pooling aggregates information from a large number of inputs into increasingly sparse spatial structures.

Besides the different structure levels, differences in protein sizes require special consideration, as no deep analysis on a single resolution will be able to process all real-world proteins as a whole. Unfortunately, not even the most basic pooling operation to reduce the many pixels making up an image for classification [30] has an obvious pendant when it comes to protein structures. We could simply pool using the extrinsics, such as by farthest point sampling [41], Poisson disk [22], or using grids [2, 43], but it is unclear what the intrinsics of that new representation would be. While the laws of physics determine how atoms exchange electrons, they cannot answer what the intrinsics of a simplified graph representation would be. Due to folding, two atoms might come close in space, yet they should not merge.

We therefore exploit the fact that proteins are a recombination of a finite set of n_a amino acids, whereby typically $n_a = 20$ holds when considering the proteinogenic or natural amino acids encoded through DNA. Hence, pooling for proteins is neither as simple as for structured images (one pooling rule), nor as complex as for unstructured graphs (arbitrary number of pooling rules), but semi-structured. We therefore suggest operating in two steps: we first learn n_a independent pooling operations (Sec. 5.1), i. e., graph clusterings, one for every type of amino acid. In a second step (Sec. 5.2), when learning – or later testing – on complex proteins, we segment the protein into amino acids and apply the clustering to each amino acid until the topology is regular, followed by regular pooling. We will detail both steps in the following sections.

5.1 Clustering

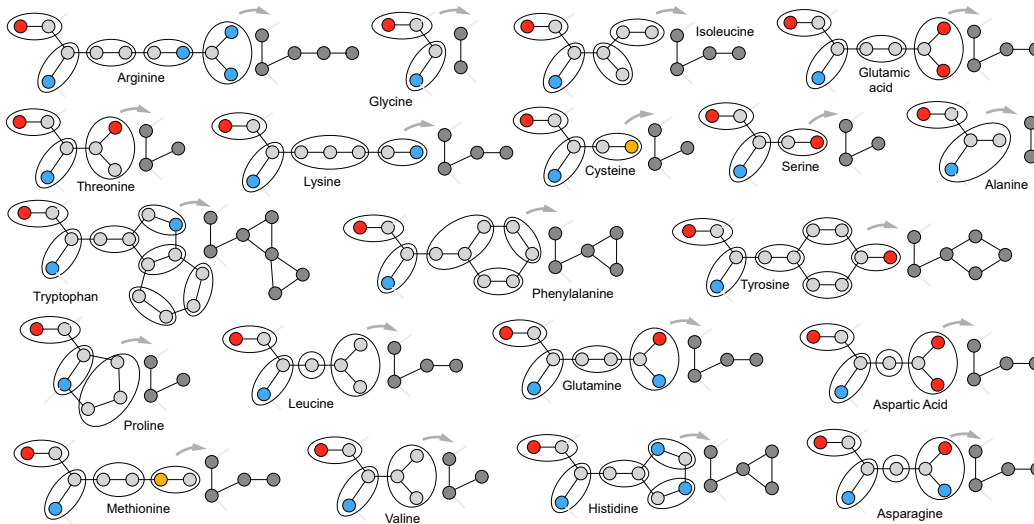


Figure 3: One-level clustering of the 20 canonical amino acids. For each pair we show the amino acid on the left and the clustering on the right.

Clustering is applied to each type of amino acid individually. For the i -th type of amino acid, we first collect the adjacency matrix A_i of its bonds' structure. We next run multiple steps of clustering to produce a sequence of clustering matrices $C_{i,j}$, whereby in each iteration, we use the clustering to halve the number of nodes. While we use spectral clustering [48], any clustering method that accepts distance matrices as inputs, such as k-medoids [40], could be used. Fig. 3 shows the resulting pooling.

When building adjacency, we only consider bonds that are local to the amino acid and ignore those bonds that are not. The pooling proposed in the next sub-section will nonetheless be able to preserve the bonds ignored, just without optimizing for them in the clustering.

Our clustering has no learnable parameters. It is found once for every amino acid, independent of the task. This allows sharing the pooling across all occurrences of amino acids of a protein, as well as across tasks. It replaces the regular pooling topology, e. g., 2×2 in images [30], which is differentiable, but not learned either. Please note the similarity between sharing pooling masks in our work and sharing filter weights in CNNs.

5.2 Pooling



Figure 4: Hierarchical protein pooling: **(a)** We segment the protein into amino acids (blue, orange, green), and the backbone (grey). Edges represent two types of bonds: solid ones for covalent bonds and dotted edges for hydrogen bonds. **(b)** Each type of amino acid is clustered in the same way. **(c)** Each resulting amino acid is pooled to its carbon- α , linked to the backbone, which results in a chain topology **(d)**. **(e)** A chain is easy to pool, arriving at the scalar result **(f)**.

Pooling is applied to an entire protein when learning or testing.

First (Fig. 4, a), we segment the protein into amino acids.

Second (Fig. 4, b), we apply the cluster matrices to every amino acid instance and the features of the new node are computed as the average of the collapsed atoms. Bonds (dotted edges in Fig. 4) that connect atoms of different amino acids (e. g., hydrogen bonds) are treated like any other edge: when nodes merge into one, these edges are also merged to link to that node. Recall that the clustering rules ignored those bonds. In Fig. 4 (a), one atom in one instance of the blue amino acid, is linked to the only atom in the green amino acid. The other instance of the blue amino acid type is not linked. The clustering is applied regardless, “transferring” the external edge from the collapsing to the collapsed atom.

Third (Fig. 4, c), the last clustering is an average-pooling to the carbon- α that is present in every amino acid to connect the residue to the backbone.

Now, the graph has the topology of a set of chains. All following pooling operations (Fig. 4, d and e) simply remove every second node in each chain and assign the average of the remaining node and the connected removed nodes to the remaining node. After a fixed number of poolings, a global aggregation with a symmetric function results in a single value (Fig. 4, f).

6 Evaluation

To evaluate ProteiNN, we specify a deep architecture (Sec. 6.1) to be compared to other published methods (Sec. 6.2) as well as different ablations (Sec. 6.3) of our approach. During our evaluation, we focus on three common protein classification tasks in Sec. 6.4, Sec. 6.5, and Sec. 6.6.

6.1 Our Architecture

By facilitating multi-graph convolution and pooling, we can realize a deep architecture that is suited for learning on complex proteins. Similar to what is common practice when learning on images, we therefore combine the proposed convolution and pooling to address protein analysis tasks.

Atom features are 6D and comprise 1) chemical element code, 2) covalent radius, 3) van der Waals radius, and 4) atom mass. Chemical elements are provided as one-hot codes \mathbf{c} for the n_e different chemical elements found in proteins. These codes are embedded into n_h -dimensional (we choose $n_h = 3$) vector codes $\mathbf{h} = \mathbf{H}\mathbf{c}$ by learning a matrix $\mathbf{H} \in \mathbb{R}^{n_e \times n_h}$.

Five layers of two ResNet [19] bottleneck blocks each of intrinsic-extrinsic convolutions follow. All convolution kernels are MLPs [22] with one layer, 16 hidden neurons, and a leaky ReLU. The first convolution with a receptive field of 3 angstroms (\AA) maps from 6D to 64D, followed by the clustering pooling. The second convolution (receptive field 6\AA) produces 128D, followed by

pooling to the carbon- α . The third, fourth, and fifth convolution (receptive fields 8 Å, 12 Å, and 16 Å) double the feature count to 256, 512, and 1024 respectively, each followed by regular topology backbone pooling. The size of the receptive fields in each level has been chosen to include an almost constant number of atoms in it. Note that atoms not belonging to an amino acid are removed in a pre-processing step, however, these can contribute to the convolutions of the first level if necessary.

As the architecture is fully-convolutional, it can process proteins of arbitrary size, but after finitely many (we choose five) steps, also obtains an intermediate result of varying size. Hence, to reduce this to one final result vector, a symmetric aggregation operation, average, is used.

We use cross entropy loss, .5 dropout for internal and .2 for convolutions and momentum optimization with an initial learning rate of .001 which is decreased over training.

6.2 Other Architectures

We compare our results to GCNN [27] and a hierarchical variant, EdgePool [9], composed of 3 convolution layers followed by a global Readout operation after each. These methods consider as input protein graphs, in which nodes are amino acids and edges are defined by a spatial distance of 8 Å. As initial node features, we learn a 64 D amino acid embedding similar to the one learned by our architecture for each atom type. We also compare to 1D CNNs [47, 31, 32], which define the protein as a sequence of 3-gram overlapping amino acids and applies 3 convolutional layers before a global pooling. Lastly, we compare to 3D CNNs [8, 2], which uses a 64^3 3 D discretization of the space containing the protein with voxels size of 1.5 Å. The inputs are the 11 channels described in Derevyanko et al. [8] followed by 6 layers of a residual block plus max pooling. We retrained all methods with the optimization settings stated above.

6.3 Ablations of Our Method

We study four axes of ablation: *convolution*, *neighborhood*, *pooling*, and *representation*. When moving along one axis, all other axes are fixed to Ours (●).

Convolution ablation. We consider four different ablations of convolutions. Graph Convolutional Neural Networks, denoted as GCNN (○), only aggregate, for each node, the dot product of a learned vector with all node features in the neighborhood, as also proposed by others [27, 18]. In particular, we use the aggregation function proposed by Kipf and Welling [27]. This ablation resembles graph convolutions [20, 38] previously used to learn on molecular data [11, 26, 15]. In ExConv (◐), convolutions are based on kernels defined in 3 D space only [41, 22], without taking into account intrinsic distances. Symmetrically, we study three further variants using only the intrinsic distances. InConvC (◑) uses only geodesics on the covalent bond graph \mathcal{E}_1 , while InConvH (◒) uses geodesics on the covalent+hydrogen bond graph \mathcal{E}_2 . Lastly, InConvCH (◓) makes use of both geodesics at the same time. We present two variants of our intrinsic-extrinsic convolution. Ours3DCH (◔) used both geodesics plus distances along the three spatial dimensions, and Ours (●) refers to our proposed intrinsic-extrinsic convolution which uses both geodesics plus Euclidean distance.

Neighborhood ablation. We compare several methods to define our receptive field: CovNeigh (◕), which uses distances on graph \mathcal{E}_1 , HyNeigh (◖), which uses distances on graph \mathcal{E}_2 , as well as Ours (●) which uses distances in 3 D space.

Pooling ablation. We consider four options. GridPool (◗) overlays the protein with increasingly coarse grids and pools all atoms into one cell [45]. Some work has suggested to learn pooling for graphs [51, 33, 35]. To this end, TopKPool (◘) learns a per-node [14] and EdgePool (◙) a per-edge importance score [9] which is used to drop nodes or remove edges. In both cases, we first pool atoms, next cluster to carbon α and then cluster the backbone. Our pooling is included as Ours (●).

Representation ablation. As ProteiNN works on the atom level, we have also analyzed how this representation compares to a representation on the granularity of amino acids instead, as it is used by others [16, 51, 14]. We will denote this ablation as AminoGraph (◚) in comparison to Ours (●).

Table 2: Study of ablations (rows) for the fold and reaction tasks (columns).

		FOLD task		REACTION task		
		Inter	Intra	Inter	Intra	
Convolution	GCNN	76.7 %	75.7 %	84.9 %	78.2 %	
	ExConv	80.8 %	79.3 %	85.0 %	78.2 %	
	InConvC	83.1 %	81.3 %	85.4 %	79.0 %	
	InConvH	84.4 %	82.1 %	85.5 %	78.6 %	
	InConvCH	86.4 %	84.1 %	85.2 %	78.6 %	
	Ours3DCH	86.6 %	83.8 %	85.8 %	79.6 %	
	Ours	87.4 %	84.5 %	87.2 %	81.1 %	
Neighbors	CovNeigh	70.6 %	68.9 %	41.6 %	35.1 %	
	HyNeigh	79.4 %	76.4 %	56.9 %	48.8 %	
	Ours	87.4 %	84.5 %	87.2 %	81.1 %	
Pool	GridPool	82.0 %	80.7 %	86.1 %	79.9 %	
	TopKPool	80.1 %	77.1 %	84.5 %	77.4 %	
	EdgePool	87.4 %	84.3 %	86.9 %	81.4 %	
	Ours	87.4 %	84.5 %	87.2 %	81.1 %	
Representation	AminoGraph	86.4 %	84.1 %	85.3 %	78.5 %	
	Ours	87.4 %	84.5 %	87.2 %	81.1 %	

6.4 Task 1: Enzyme-no-Enzyme Classification (ENZYME)

Task. This is a binary classification of an entire protein into either being an enzyme or not. Despite the fact that this task is rather simple as compared to our other tasks, we have included it, as it has been extensively used as a benchmark for graph classification methods [39].

Dataset. We use the 1,173 proteins that contain atomic information in the Protein Data Bank (PDB) [4] from the dataset defined by Dobson and Doig [10], with $k = 10$ -fold cross-validation.

Results. Tbl. 1 presents comparisons in which our method outperforms all competing methods. We further see that the gap is widening as tasks get more complex: while on the ENZYME task, other approaches are in the same regime, more involved tasks related to spatial arrangement such as FOLD and REACTION, to be introduced next, are not solved successfully by other techniques.

6.5 Task 2: Fold Classification (FOLD)

Task. A protein’s fold refers to its overall architecture, based on which proteins are classified into different fold classes. In this task, given a protein, we predict the fold class [37], whereby performance is measured as inter-class and intra-class accuracy. The inter-class accuracy (sometimes referred to as “micro” accuracy) is the mean accuracy across all classes. For robustness to class imbalance, we also report the mean of the means of each class (sometimes denoted as “macro” accuracy).

Dataset. We selected 100 different folds from the SCOPe database and collected 44, 685 protein domains (around 500 per fold class). These were split into 37, 136 protein domains for training, 1, 847 for validation, and 5, 702 for testing. We ensured that all proteins in each set has less than 55 % sequence similarity to all proteins in the other sets, allowing for proper evaluation of the generalization of the methods tested. A full description of the dataset is provided in the supplementary material.

Table 1: Comparison to other methods on the three tasks.

Task→	ENZYME	FOLD		REACTION	
		Inter	Intra	Inter	Intra
GCNN	81.7 %	39.8 %	39.8 %	64.6 %	52.1 %
EdgePool	81.5 %	41.6 %	43.4 %	63.2 %	52.8 %
1D CNN	75.5 %	31.1 %	30.4 %	60.6 %	48.1 %
3D CNN	81.2 %	63.0 %	63.2 %	68.5 %	60.7 %
Ours	86.9 %	87.4 %	84.5 %	87.2 %	81.1 %

Results. Results, as compared to other methods, are also reported in Tbl. 1. We find our method to perform better by a large margin according to both metrics. Tbl. 2 shows how the tested ablations perform on this task, whereby some of these ablations resemble previous work. Overall we see that Ours (●) performs better than any ablation, most by a substantial margin, indicating that our protein-specific representation, convolution, and pooling are all important ingredients. The EdgePool (●) ablation performs en-par with our approach according to some metrics, however note that this only uses Diehl’s [9] pooling, combined with all other components we propose. The performance of [9] alone is not to be seen as competitive in this task at Tbl. 1.

In Tbl. 3 we look at the fold classification accuracy of our method compared to non-learning-based techniques and the computation time for our full test set (5.7 K proteins). Our method has much better accuracy than BLAST [1] and performs orders of magnitude faster than TMAAlign [53], while having an increase of inter-class accuracy of 0.5 % and only a drop of intra-class accuracy of 1.7 %.

We also verified that pooling is stable under the initialization of the clustering. When seeding the spectral clustering randomly, the variance for FOLD is .02 % relative to the mean 87.4 % of our method for FOLD and .013 %, respectively, for the mean 87.2 % for REACTION, both for “Inter”, in Tbl. 2.

Table 3: Performance and computation speed for our method and non-learned methods on the FOLD task.

	Inter	Intra	Time
BLAST	45.6 %	46.6 %	249.6 s
TMAAlign	86.9 %	86.2 %	71.8 h
Ours	87.4 %	84.5 %	17.5 s

6.6 Task 3: Enzyme-Catalyzed Reaction Classification (REACTION)

Task. For this task, we classify proteins based on the enzyme-catalyzed reaction according to all four levels of the Enzyme Commission (EC) number [49]. Performance is again evaluated as the inter- and intra-class mean accuracy.

Dataset. We collected a total of 37, 428 proteins from 384 EC numbers. The data was then split into 29, 215 instances for training, 2, 562 instances for validation, and 5, 651 for testing. Note that all proteins have less than 50% sequence-similarity in between splits. Unlike the fold classification dataset, this has highly unbalanced classes due to the low number of annotated chains for some of the EC numbers, which makes this task even more challenging. A full description of the dataset is provided in the supplementary material.

Results. Again, our method outperforms previous work on this task by a large margin (Tbl. 1). Ablations of our method for this task (Tbl. 2) give further indication that all our components are relevant also for other tasks. Previous work has aimed to predict only the coarsest level of the hierarchy [5, 2], while we predict the full EC number as in Gligorijevic et al. [16]. Note how the network has to predict protein functions from the 3 D structure.

In Fig. 5, we compare additional memory required to represent the first layer of the network for a single batch of eight elements (assuming the maximum number of atoms per protein on the dataset, 28.9 K) against accuracy. Fig. 5 also presents the required time to process the complete test set (5.6 K proteins) compared with the achieved accuracy. Our method is the fastest among the presented methods, obtaining a higher accuracy within the same time.

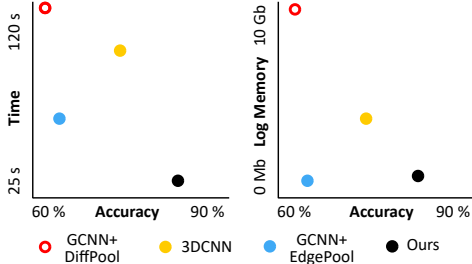


Figure 5: Execution time for the test set and additional memory required for the first layer, for different methods on the enzyme-catalyzed reaction classification task.

7 Conclusions

Based on the multi level structure of proteins, we have proposed a scalable neural network architecture for deep protein analysis. The presented architecture takes advantage of the protein primary, secondary, and tertiary structure to learn a convolution operator that works with intrinsic and extrinsic distances

as input. Moreover, we have presented a set of pooling operations that enable the dimensionality reduction of the input mimicking the designs used by convolutional neural networks on images.

Our designs lead to a new state-of-the-art performance on several relevant tasks for protein analysis, such as protein fold or enzyme-catalytic reaction classification, outperforming current approaches.

In the future, we see several opportunities for extending our work. A clear follow-up work would be to design an encoder-decoder architecture in order to perform predictions at atomic or amino acid levels. Another future direction is the development of training algorithms for this specific type of data that takes into account the inherent noise on the available annotations.

References

- [1] S. Altschul, W. Gish, W. Miller, E. Myers, and D. Lipman. Basic local alignment search tool. *J Molecular Biology*, 215(3):403–10, 1990.
- [2] A. Amidi, S. Amidi, D. Vlachakis, V. Megalooikonomou, N. Paragios, and E. Zacharaki. EnzyNet: enzyme classification using 3D convolutional neural networks on spatial representation. *arXiv:1707.06017*, 2017.
- [3] M. Atzmon, H. Maron, and Y. Lipman. Point convolutional neural networks by extension operators. *arXiv:1803.10091*, 2018.
- [4] H. M. Berman, J. Westbrook, Z. Feng, G. Gilliland, T. N. Bhat, H. Weissig, I. N. Shindyalov, and P. E. Bourne. The Protein Data Bank. *Nucleic Acids Res*, 28(1):235–42, 01 2000.
- [5] K. M. Borgwardt, C. S. Ong, S. Schoenauer, S. V. N. Vishwanathan, A. J. Smola, and H. P. Kriegel. Protein function prediction via graph kernels. *Bioinformatics*, 21(1), 2005.
- [6] L. Brocchieri and S. Karlin. Protein length in eukaryotic and prokaryotic proteomes. *Nucleic Acids Res*, 33(10):3390–400, 2005.
- [7] J. M. Dana, A. Gutmanas, N. Tyagi, G. Qi, C. O’Donovan, M. Martin, and S. Velankar. SIFTS: updated Structure Integration with Function, Taxonomy and Sequences resource allows 40-fold increase in coverage of structure-based annotations for proteins. *Nucleic Acids Research*, 47: D482–D489, 11 2018. doi: 10.1093/nar/gky1114.
- [8] G. Derevyanko, S. Grudinin, Y. Bengio, and G. Lamoureaux. Deep convolutional networks for quality assessment of protein folds. *Bioinformatics*, 34(23):4046–53, 2018.
- [9] F. Diehl. Edge contraction pooling for graph neural networks. *arxiv:1905.10990*, 2019.
- [10] P. D. Dobson and A. J. Doig. Distinguishing enzyme structures from non-enzymes without alignments. *J Molecular Biology*, 330(4):771–783, 2003.
- [11] D. K. Duvenaud, D. Maclaurin, J. Iparraguirre, R. Bombarell, T. Hirzel, A. Aspuru-Guzik, and R. P. Adams. Convolutional networks on graphs for learning molecular fingerprints. In *NIPS*, pages 2224–2232, 2015.
- [12] D. C. Elton, Z. Boukouvalas, M. D. Fuge, and P. W. Chung. Deep learning for molecular design—a review of the state of the art. *Molecular Systems Design & Engineering*, 4(4):828–49, 2019.
- [13] M. Finzi, S. Stanton, P. Izmailov, and A. G. Wilson. Generalizing convolutional neural networks for equivariance to lie groups on arbitrary continuous data. *arXiv:2002.12880*, 2020.
- [14] H. Gao and S. Ji. Graph U-nets. In *ICML*, pages 2083–2092, 2019.
- [15] J. Gilmer, S. S. Schoenholz, P. F. Riley, O. Vinyals, and G. E. Dahl. Neural message passing for quantum chemistry. In *ICML*, pages 1263–1272, 2017.
- [16] V. Gligorijevic, P. D. Renfrew, T. Kosciolk, J. K. Leman, K. Cho, T. Vatanen, D. Berenberg, B. Taylor, I. M. Fisk, R. J. Xavier, R. Knight, and R. Bonneau. Structure-based function prediction using graph convolutional networks. *bioRxiv*, 2019.

- [17] F. Groh, P. Wieschollek, and H. P. A. Lensch. Flex-convolution (million-scale point-cloud learning beyond grid-worlds). In *ACCV*, 2018.
- [18] W. Hamilton, Z. Ying, and J. Leskovec. Inductive representation learning on large graphs. In *NIPS*, pages 1024–34, 2017.
- [19] K. He, X. Zhang, S. Ren, and J. Sun. Deep residual learning for image recognition. In *2016 IEEE Conference on Computer Vision and Pattern Recognition (CVPR)*, pages 770–778, 2016.
- [20] M. Henaff, J. Bruna, and Y. LeCun. Deep convolutional networks on graph-structured data. *arXiv:1506.05163*, 2015.
- [21] L. Hermansson, F. D. Johansson, and O. Watanabe. Generalized shortest path kernel on graphs. In *Int Conf Discovery Science*, pages 78–85, 2015.
- [22] P. Hermosilla, T. Ritschel, P.-P. Vazquez, A. Vinacua, and T. Ropinski. Monte carlo convolution for learning on non-uniformly sampled point clouds. *ACM Trans. Graph. (Proc. SIGGRAPH Asia)*, 37(6), 2018.
- [23] H. Hoppe. Progressive meshes. In *Proc. SIGGRAPH*, pages 99–108, 1996.
- [24] J. Ingraham, V. Garg, R. Barzilay, and T. Jaakkola. Generative models for graph-based protein design. In *NeurIPS*, pages 15820–15831, 2019.
- [25] J. Jiménez, S. Doerr, G. Martínez-Rosell, and A. S. Rose. DeepSite: protein-binding site predictor using 3D-convolutional neural networks. *Bioinformatics*, 33(19):3036–3042, 2017.
- [26] S. Kearnes, K. McCloskey, M. Berndl, V. Pande, and P. Riley. Molecular graph convolutions: moving beyond fingerprints. *J Computer-aided Molecular Design*, 30(8):595–608, 2016.
- [27] T. N. Kipf and M. Welling. Semi-supervised classification with graph convolutional networks. *ICML*, 2017.
- [28] J. Klicpera, J. Groß, and S. Günnemann. Directional message passing for molecular graphs. *ICLR*, 2020.
- [29] B. Knyazev, X. Lin, M. R. Amer, and G. W. Taylor. Spectral multigraph networks for discovering and fusing relationships in molecules. *NIPS Workshop on Machine Learning for Molecules and Materials*, 2018.
- [30] A. Krizhevsky, I. Sutskever, and G. E. Hinton. Imagenet classification with deep convolutional neural networks. In *NIP*, pages 1097–1105, 2012.
- [31] M. Kulmanov and R. Hoehndorf. DeepGOPlus: improved protein function prediction from sequence. *Bioinformatics*, 36(2):422–429, 2019.
- [32] M. Kulmanov, M. A. Khan, and R. Hoehndorf. DeepGO: predicting protein functions from sequence and interactions using a deep ontology-aware classifier. *Bioinformatics*, 34(4):660–668, 2017.
- [33] J. Lee, I. Lee, and J. Kang. Self-attention graph pooling. In *ICML*, 2019.
- [34] S. Liu, M. F. Demirel, and Y. Liang. N-Gram Graph: Simple unsupervised representation for graphs, with applications to molecules. In *NIPS*, pages 8466–8478, 2019.
- [35] Y. Ma, S. Wang, C. C. Aggarwal, and J. Tang. Graph convolutional networks with eigenpooling. In *Proc. Int. Conf. Knowledge Discovery & Data Mining*, 2019.
- [36] C. Morris, M. Ritzert, M. Fey, W. L. Hamilton, J. E. Lenssen, G. Rattan, and M. Grohe. Weisfeiler and Leman go neural: Higher-order graph neural networks. In *Proc. AAAI*, 2019.
- [37] A. Murzin, S. Brenner, T. Hubbard, and C. Chothia. SCOP: a structural classification of proteins database for the investigation of sequences and structures. *J Mol Biol.*, 247(4):536–540, 1995.
- [38] M. Niepert, M. Ahmed, and K. Kutzkov. Learning convolutional neural networks for graphs. In *ICML*, pages 2014–23, 2016.

- [39] Papers With Code. URL paperswithcode.com/sota/graph-classification-on-dd. Accessed on 1.6.2020.
- [40] H.-S. Park and C.-H. Jun. A simple and fast algorithm for k-medoids clustering. *Expert systems with applications*, 36(2):3336–3341, 2009.
- [41] C. R. Qi, H. Su, K. Mo, and L. J. Guibas. PointNet: Deep learning on point sets for 3D classification and segmentation. *CVPR*, 2017.
- [42] C. R. Qi, L. Yi, H. Su, and L. J. Guibas. PointNet++: Deep hierarchical feature learning on point sets in a metric space. *NIPS*, 2017.
- [43] M. Ragoza, J. Hochuli, E. Idrobo, J. Sunseri, and D. R. Koes. Protein–ligand scoring with convolutional neural networks. *J Chemical Information and Modeling*, 57(4):942–957, 2017.
- [44] O. Ronneberger, P. Fischer, and T. Brox. U-net: Convolutional networks for biomedical image segmentation. In *MICCAI*, volume 9351 of *LNCS*, pages 234–241, 2015.
- [45] H. Thomas, C. R. Qi, J.-E. Deschaud, B. Marcotegui, F. Goulette, and L. J. Guibas. KPConv: Flexible and deformable convolution for point clouds. *ICCV*, 2019.
- [46] R. Townshend, R. Bedi, P. Suriana, and R. Dror. End-to-end learning on 3D protein structure for interface prediction. In *NeurIPS*, pages 15642–15651, 2019.
- [47] M. Tsubaki, K. Tomii, and J. Sese. Compound–protein interaction prediction with end-to-end learning of neural networks for graphs and sequences. *Bioinformatics*, 35(2):309–318, 2018.
- [48] U. von Luxburg. A tutorial on spectral clustering. *Statistics and computing*, 17(4):395–416, 2007.
- [49] E. C. Webb. *Enzyme Nomenclature 1992*. Academic Press, 1992.
- [50] Z. Wu, S. Pan, F. Chen, G. Long, C. Zhang, and P. S. Yu. A comprehensive survey on graph neural networks. *IEEE Trans Neural Networks and Learning Systems*, 2020.
- [51] Z. Ying, J. You, C. Morris, X. Ren, W. Hamilton, and J. Leskovec. Hierarchical graph representation learning with differentiable pooling. In *NIPS*, pages 4800–4810, 2018.
- [52] J. You, R. Ying, and J. Leskovec. Position-aware graph neural networks. In *ICML*, pages 7134–43, 2019.
- [53] Y. Zhang and J. Skolnick. Tm-align: a protein structure alignment algorithm based on the tm-score. *Nucleic Acids Res*, 33(7):2302–2309, 2005.
- [54] Z. Zhang, C. Dongdong, J. Wang, L. Bai, and E. Hancock. Quantum-based subgraph convolutional neural networks. *Pattern Recognition*, 88:38–49, 2018.

Supplementary material

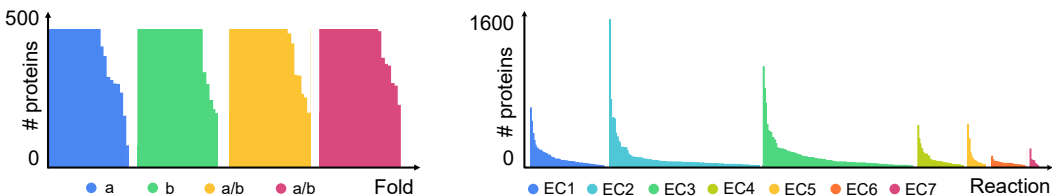


Figure 6: Histogram of the data sets for FoLd classification (left) and enzyme-catalyzed Reaction classification (right). The left histogram is color-coded by the Class of each FoLd based on the first level of the SCOPe database [37] classification hierarchy. The right histogram is color-coded by the higher classification level of the Enzyme Commission number [49].

A Datasets

A.1 Fold classification

In order to evaluate the performance of our network classifying proteins on different folds we collected protein domains from the SCOPe database [37]. This database classifies protein domains into a hierarchical structure: Class \rightarrow Fold \rightarrow Superfamily \rightarrow Family \rightarrow Protein \rightarrow Species. From each of the four first Classes, (*a*: All alpha proteins, *b*: All beta proteins, *c*: Alpha and beta protein (*a/b*), and *d*: Alpha and beta proteins (*a+b*)) we selected the 25 Folds that contained more protein domains. From each of those, we randomly selected 500 protein domains (when available) to represent the FoLd. This resulted in 44,685 protein domains in total (Fig. 6 presents and histogram of the number of protein domains per FoLd).

The dataset was divided into three sets, training, validation, and testing. For each FoLd, we selected 30% of the Families for validation and testing and 70% for training. Note that protein domains from different Families have 55% or less sequence similarity. From the Families selected for validation and testing, 25% were selected for validation and 75% for testing. This resulted in 37,136 protein domains for training, 1,847 for validation, and 5,702 for testing.

A.2 Enzyme-Catalyzed Reaction Classification

We downloaded Enzyme Commission number (EC) [49] annotations from the SIFTS database [7]. This database contains EC annotations for entries on the Protein Data Bank (PDB) [4]. From the annotated enzymes we cluster their protein chains using a 50% sequence similarity threshold, as provided by PDB [4]. We selected the unique complete EC numbers (e.g. EC 3.4.11.4) for what five or more unique clusters were annotated with it. For each cluster, we selected five different proteins (less than 100% sequence similarity among them) as representatives. Note that even if the proteins are similar, selecting several chains per cluster can be understood as a type of data augmentation. In total, we collected 37,428 annotated protein chains (Fig. 6 presents and histogram of the number of protein chains per Enzyme type). Due to the low number of annotations for some of the enzyme types, the resulting data set contains high unbalanced number of protein chains per EC number.

Lastly, we split the data set into three sets, training, validation, and testing, ensuring that every EC number was represented in each set and all protein chains belonging to the same cluster are in the same set. This resulted in 29,215 protein chains for training, 2,562 protein chains for validation, and 5,651 for testing.